Localization transition in a ballistic quantum wire

H. Steinberg,[1] O. M. Auslaender,[1,*] A. Yacoby,[1] J. Qian,[2] G. A. Fiete,[2,3] Y. Tserkovnyak,[2] B. I. Halperin,[2] K. W. Baldwin,[4] L. N. Pfeiffer,[4] and K. W. West[4]

[1]*Department of Condensed Matter Physics, Weizmann Institute of Science, Rehovot 76100, Israel*
[2]*Lyman Laboratory of Physics, Harvard University, Cambridge, Massachusetts 02138, USA*
[3]*Kavli Institute for Theoretical Physics, University of California, Santa Barbara, California 93106, USA*
[4]*Bell Labs, Lucent Technologies, 700 Mountain Avenue, Murray Hill, New Jersey 07974, USA*

(Received 26 January 2006; published 10 March 2006)

The many-body wave function of localized states in one dimension is probed by measuring the tunneling conductance between two parallel wires, fabricated in a GaAs/AlGaAs heterostructure. Tunneling conductance in the presence of a magnetic field perpendicular to the plane of the wires serves as probe of the momentum space wave function of the wires. One of the two wires is driven into the localized regime using a density tuning gate, whereas the other wire, still in the regime of extended electronic states, serves as a momentum spectrometer. As the electron density is lowered to a critical value, the state at the Fermi level abruptly changes from an extended state with a well-defined momentum to a localized state with a wide range of momentum components. The signature of the localized states appears as discrete tunneling features at resonant gate voltages, corresponding to the depletion of single electrons and showing Coulomb-Blockade behavior. Typically 5–10 such features appear, where the one-electron state has a single-lobed momentum distribution, and the few-electron states have double-lobed distributions with peaks at $\pm k_F$. A theoretical model suggests that for a small number of particles ($N<6$), the observed state is a mixture of ground and thermally excited spin states.

DOI: 10.1103/PhysRevB.73.113307 PACS number(s): 73.21.Hb, 73.20.Qt, 73.23.Ad

Coulomb interactions in many-body quantum systems can lead to the creation of exotic phases of matter. A prime example is a Luttinger liquid, which describes a system of interacting electrons confined to one spatial dimension.[1] At high electron densities the electron kinetic energy dominates over the Coulomb energy and the transport properties of the system resemble those of noninteracting electrons. In this weakly interacting limit, conductance is quantized even in the presence of moderate disorder.[2,3] Reducing the electron density suppresses the kinetic energy more rapidly than the Coulomb energy, leading to the strongly interacting limit, where charge correlations resemble those in a Wigner crystal, an ordered lattice of electrons with periodicity n^{-1} (n is the average electron density). In this limit, one expects the weakest amount of disorder to pin the crystal, thereby suppressing conductance at low temperatures.[4] In a previous work[5] we presented tunneling measurements of a wire undergoing suppression of conductance as n is reduced below a critical density. The electrons left in the wire are argued to be localized. Here we focus on these localized electrons, measuring their many-body wave function using tunneling spectroscopy between two wires, the localized wire and another extended wire.

Momentum resolved tunneling between two quantum wires has been shown to be an effective experimental tool in the study of interacting one-dimensional (1D) systems. This method uses tunneling across an extended junction between two closely situated parallel clean quantum wires.[6] An electron tunneling across the junction gets a momentum boost of $q=eBd/\hbar$ (B is the magnetic field perpendicular to the plane of the wires, d is the distance between them, as in Fig. 1). The probability for an electron to tunnel between the wires can be measured through the tunneling conductance $G_T(B)$ (taken at low, but finite bias voltage V_{SD}). At low temperatures $G_T(B) \propto |\Psi(k)|^2$,[5,7] assuming the lower wire is uniform and weakly interacting, where $\Psi(k)$ is the tunneling matrix element

$$\Psi(k) = \int_{-\infty}^{\infty} dx e^{ikx} \Psi(x), \tag{1}$$

$\Psi(x)$ is a "quasiwave function" for the upper wire, defined by: $\Psi(x)=\langle N-1|\psi(x)|N\rangle$. Here $k=q_B-k_F^L$, where k_F^U, k_F^L are the Fermi-wave number in the upper, lower wires (UW, LW). $|N\rangle$ is the ground state for N particles in the UW, and $\psi(x)$ is an operator that removes an electron from point x in the UW.[8] In the absence of interactions, $\Psi(x)$ would be the wave function of the Nth electron, which is a plane wave for an infinite system. In this case we expect $|\Psi(k)|^2 \propto \delta(k+k_F^U)$

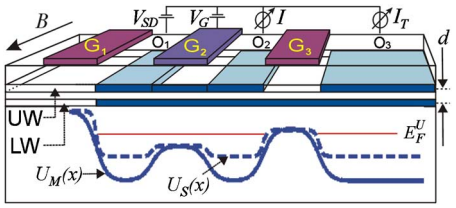

FIG. 1. (Color online) A schematic of the measurement setup with cleave plane front, perpendicular to B. Depicted: 2 μm wide top gates (G_1, G_2, and G_3), 20 nm thick upper wire at the edge of the 2DEG, 30 nm thick lower wire and 6 nm insulating AlGaAs barrier. $U_S(x)[U_M(x)]$: Schematic of UW gate-induced potentials for single-mode (multimode) wires, E_F^U is the Fermi energy of the upper wire. Ohmic contact O_1 serves as source, $O_{2,3}$ as drains. Density is controlled by gate voltage V_G. Two-terminal current is marked by I, tunneling current by I_T.

$+\delta(k-k_F^U)$. $G_T(B)$ is therefore finite only when $|B|=B^{\pm}$, corresponding to the two momentum-space δ functions, with

$$B^{\pm}=\frac{\hbar}{ed}|k_F^U \pm k_F^L| \tag{2}$$

allowing tunneling only between the Fermi points of the two wires.

The precise line shape of $G_T(B)$ gives the microscopic properties of the many-body states involved in the tunneling process: A realistic, finite size junction gives rise to fringes accompanying the δ-function peaks of $\Psi(k)$.[7] When a wire localizes, $\Psi(k)$ changes significantly and becomes spread-out in k space. In this work we report on measurements of $\Psi(k)$ of localized electrons using $G_T(B)$ as its probe.

The experimental setup is schematically drawn in Fig. 1. It is realized by two parallel wires at the edges of two quantum wells fabricated in a GaAs/AlGaAs heterostructure by cleaved edge overgrowth (CEO).[9] Only the top quantum well (0.5 μm deep) is populated by a two-dimensional electron gas (2DEG) which serves as a contact to the UW through Ohmic contacts $O_{1,2,3}$. The experiment is set up using 2 μm wide tungsten gates on the top surface $G_{1,2,3}$: G_3 is set to a negative voltage where the UW is depleted and LW remains continuous, so that only the tunneling current is measured between source O_1 and drain O_3. G_1 is set to deplete both wires, so that the tunneling junction at the drain is much longer than the one at the source, ensuring that the LW is kept at drain potential. The density of a segment in the wire is varied by applying voltage V_G to G_2. Contact O_2 may be set to either the source or drain voltage to allow simultaneous reading of two-terminal UW conductance and tunneling conductance. The density-dependent measurement consists of setting B and measuring the tunneling current $I_T=G_TV_{SD}$ as a function of V_G. The tunneling current includes contributions which are not V_G dependent. To single out the density-dependent contribution, the differential tunneling conductance dG_T/dV_G is measured using a lock-in. Typically dV_G is a few millivolts with a 4 Hz frequency. The measurements are performed in a ^{3}He refrigerator at temperatures down to 0.25 K.

Initially a cooled sample has one populated subband in the UW (henceforth "single-mode wire"). The potential landscape along the UW is marked by $U_S(x)$ in Fig. 1, where the depletion of the wire requires a relatively small negative gate voltage (−0.9 V). Illuminating the sample with infrared light increases the electron density in the wire, allowing further population of higher subbands ("multimode wire"). Depletion of the wire after illumination requires a larger (−3.5 V) gate voltage. The finite slope in $U_M(x)$ results in a shorter effective length of the low-density region.

Figure 2(a) shows the measurement of dG_T/dV_G for a single-mode wire. The figure is dominated by a set of curves marked $B^{\pm}(V_G)$. The upper curve $B^{+}(V_G)$ corresponds to the + sign in Eq. (2) and is the measured differential conductance which results from tunneling between counterpropagating states. The lower curve corresponds to the − sign in Eq. (2) which in turn results from tunneling between copropagating states. Each curve is accompanied by finite size fringes

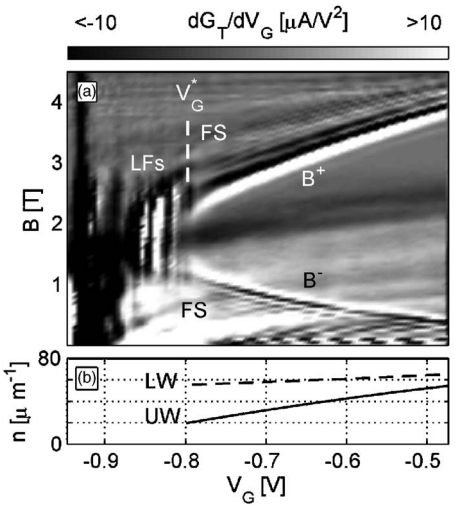

FIG. 2. (a) Plot of dG_T/dV_G vs V_G and B for a single-mode wire. Applied bias $V_{SD}=100$ μV selected to avoid the zero-bias anomaly (Ref. 10), but is small enough to consider tunneling between the Fermi points of both wires. The upper and lower curves are momentum conserving tunneling features $B^{\pm}(V_G)$. Each curve is accompanied by finite size features marked by "FS". At low densities LFs appear instead of these curves. V_G^* marks the localization transition. (b) UW and LW densities extracted using Eq. (2).

(FS) which are a consequence of the finite length of the low-density region. As the top-gate voltage grows more negative the density under the gate is reduced and the curves converge. Panel (b) shows the densities in both wires as extracted using Eq. (2).

An abrupt change in dG_T/dV_G is evident in Fig. 2 at a critical gate-voltage $V_G^*=-0.80$ V, which corresponds to a critical UW density $n^*=20$ μm^{-1}. At n^* the high density features $B^{\pm}(V_G)$ disappear, giving way to a different set of features labeled localization features (LFs). This is a fundamental change: When $n>n^*$, the charge density is uniform in the density-tuned region, and momentum is a good quantum number. dG_T/dV_G is therefore appreciable only in a narrow range of $\hbar/edL_U$ around $B^{\pm}$, L_U being the length of the density-tuned region. When $n<n^*$, the momentum range spanned by the LFs is typically very broad and lies roughly between the extrapolations of the $B^{\pm}(V_G)$ curves. Further attesting to the importance of this transition, we note that simultaneous reading of I and I_T shows that this change is concurrent with the suppression of the two-terminal conductance.[5]

The broad momentum spectrum exhibited by the LFs may have several possible interpretations. For example, $\Psi(x)$ may be localized on a length scale not much larger than the interparticle separation. Alternatively, broad LFs may result either from nonuniform density which gives rise to a broad distribution of local Fermi wave vectors, or from contributions from tunneling into excited states, where momentum may be shared by several excitations.

The central result of this work is contained in Fig. 3 where high-resolution scans of single-mode and multi-mode wire LFs are presented [panels (a) and (b), respectively]. The LFs appear as vertical streaks in B. They are narrow in the

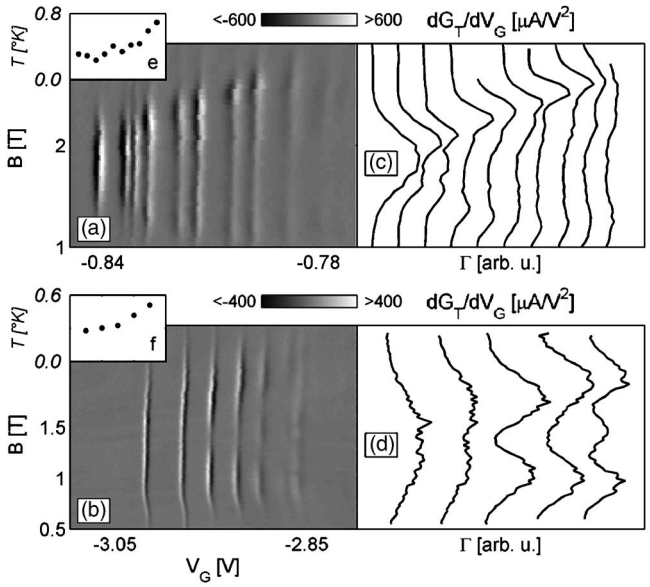

FIG. 3. (a) High resolution measurement of dG_T/dV_G of localization features for a single-mode wire, $V_{SD}=50\ \mu$V, $dV_G=300\ \mu$V. (b) Same as (a), taken for the second subband in a multimode wire. (c) $\Gamma(B)\propto|\Psi(k)|^2$ Extracted from panel (a). (d) $\Gamma(B)$ of panel (b). (e) $T(N)$ of panel (a), N is the number of the added electron for each LF. (f) $T(N)$ of panel (b). Γ and T are defined in the text.

V_G direction, separated by strips with vanishing signal. Such discrete behavior is a result of charge quantization typical of Coulomb blockade (CB) of electrons in a finite box. The number of the LFs for several cases is summarized in Table I.

The CB behavior, along with the observation that the UW states are localized, implies the existence of a localized region separated from the rest of the UW by tunnel barriers. This localized region forms a quantum dot with one or two leads to the UW segments which are not density controlled (depending on the coupling strength to each side), and one lead to the LW. As expected from CB physics, when a finite source-drain bias is applied (Fig. 4), the LFs split to form the well known diamonds.[11] The asymmetry of the diamonds indicates different capacitance to each lead.

We define the length of the low-density region above and below n^* as L_{ex} and L_{loc}, respectively. Both are extracted from the data: In the extended regime, $n>n^*$, finite size fringes accompany the $B^{\pm}(V_G)$ curves for values of $B<B^-(V_G)$ and $B>B^+(V_G)$, (marked by "FS" in Fig. 2). The location of the FS, outside the $B^{\pm}$ curves, implies that the electron density here has a minimum in the center of the UW,

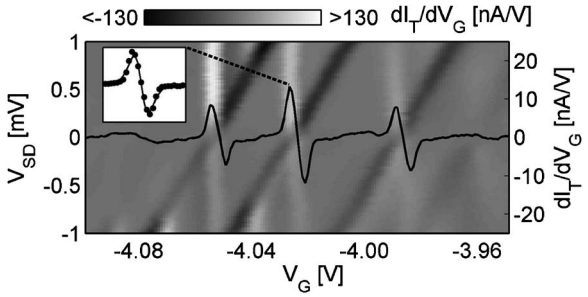

FIG. 4. dI_T/dV_G as a function of gate voltage V_G and source-drain bias V_{SD}, taken for the localization features of subband 1 in a multimode wire, at $B=2$ T. The tilted diamond features are due to resonant tunneling through the localized states. A line scan of dI_T/dV_G at a bias of 20 μV is superimposed on the plot. Inset: Second derivative of a Fermi function (line) and data (dots) of the second LF.

with a length $L_{ex}\approx 2\pi/\Delta q_B$, Δq_B being the spacing of the fringes in the B direction.[7] In the localized regime, $n<n^*$, $L_{loc}=N/n^*$, where N is the number of electrons confined to the low-density region (number of LFs). Table I summarizes the results for the LFs presented in this paper and in Ref. 5. We see that $L_{ex}/L_{loc}\approx 2$. This suggests that a sizeable fraction of the low-density region participates in the localization.

We use the LFs to extract $|\Psi(k)|^2$: A typical line scan of such LFs, taken at a constant value of B, is given in Fig. 4 along with a fit to: $\partial^2 f/\partial V_G^2=(e^2/h)\Gamma\pi/4k_BT^2\tanh(x)\cosh^2(x)$ with $x=[(\varepsilon_0-\mu)/2k_BT]$. Two adjustable parameters are used: The temperature T (in V_G units) and the tunneling rate Γ. Such fits were performed for each value of B in Fig. 3. The extracted values of Γ are presented in Figs. 3(c) and 3(d). The Coulomb-blockaded states can now be characterized by $\Gamma(B)\propto|\Psi(k)|^2$, which is a direct measure of their momentum distribution [using Eqs. (1) and (2)]. The single-mode measurement presented in panel (c) shows a generic case where $\Gamma(B)$ has a single peak for the first LF ($N=1$) and two broad peaks for $N\geqslant 2$, with a separation ΔB that increases as N is increased. There is only little variation in this behavior upon different cool downs, single versus multimode conditions and when a different gate is used. Rarely one finds momentum distribution that can be interpreted using single particle theory. Figure 3(d) shows the LFs of subband 2 in a multimode wire. One can clearly see that $N=1,2$ is approximately single-lobed, $N=3,4$ double-lobed, and $N=5$ is triple lobed. Such behavior would be expected for spin-degenerate one-dimensional electrons in a symmetric box.[8]

Insets (e) and (f) of Fig. 3 show the medians of the temperature fit for each of the LFs in (a) and (b), respectively.

TABLE I. Summary of L_{loc}, L_{ex}, N, and V_G^* for a single-mode wire and modes 1, 2 of a multimode wire.

Subband:	N	n^* (μm^{-1})	L_{loc} (μm)	L_{ex} (μm)	V_G^*
Single mode	12	20	0.6	1.0	–0.9
Multimode second	5	22	0.23		–2.6
Multimode first	6	25	0.24	0.5	–3.6

The temperature is originally obtained in units of V_G and is translated to K using the capacitance ratio measured in scans such as Fig. 4. The deduced temperature appears to increase with the addition of electrons, almost by a factor of 2. The apparent broadening of the feature cannot be explained by level broadening since the line shape does not resemble a Lorentzian. Furthermore, scans such as Fig. 4 rule out the possibility that the features broaden due to changing of lead-dot capacitance. We currently do not have a straightforward explanation for this observation.

In an attempt to model the data, we have calculated the expected tunneling form factor $|\Psi(k)|^2$ in the localized regime: For $N=1$, $\Psi(x)$ has no nodes. This agrees with the experimental results in Figs. 3(b) and 3(d). For $N=2$, however, where the spin-singlet ground state would reproduce a similar signature, the observed $\Gamma(B)$ deviates from the single-lobe structure. We therefore estimate the energy difference between the lowest triplet state and the singlet ground state for the two electron system and find it to be extremely small, less than the Zeeman energy in a field of 2 T. Mixing of the singlet-triplet states at finite temperatures reproduces the observed structure: A pair of maxima at finite $|k|$ with a nonzero local minimum at $k=0$.[8]

The energy scale for spin excitations grows rapidly with increasing density, and at $T=0.25$ K we expect spin excitations to be frozen out for $N \geqslant 5$. The estimate is sensitive to the form and size of the cutoff in the interaction potential. Calculations assuming sharp confinement lead to a form factor $|\Psi(k)|^2$ which becomes sharply peaked near $k=\pm k_F^U$. The broad peaks observed experimentally and the substantial weight near $k=0$ could be a result of softness or asymmetry in the confining potential, some residual disorder, or thermally excited spin-excitations (possibly due to the exchange energy being smaller than our estimate).[8,12,13]

In conclusion, we have studied the momentum space wave functions of localized states embedded in a quantum wire. These states appear when the wire density falls below a critical density, where the two-terminal conductance is suppressed. In this regime the localized electrons display Coulomb-blockade charging physics. Momentum spectroscopy of the localized few-electron states reveals an evolution of momentum structure from a single to a double peak.

We would like to thank R. de-Picciotto for his contribution. Y. Oreg and T. Giamarchi assisted in helpful discussions. This work was supported in part by the US-Israel BSF, the European Commission RTN Network Contract No. HPRN-CT-2000-00125, and NSF Grant Nos. DMR-02-33773 and PHY-01-17795. Y.T. is supported by the Harvard Society of Fellows. G.A.F. is supported by NSF Grant Nos. PHY-99-07949, NSF-04-57440, and by the Packard Foundation. O.M.A. acknowledges partial support from a grant from the Israeli Ministry of Science. H.S. is supported by a grant from the Israeli Ministry of Science.

*Present address: Gaballe Laboratory for Advanced Materials, Stanford University, Stanford, CA 94305, USA.

[1] F. D. M. Haldane, J. Phys. C **14**, 2585 (1981).

[2] S. Tarucha, T. Honda, and T. Saku, Solid State Commun. **94**, 413 (1995).

[3] A. Yacoby, H. L. Stormer, N. S. Wingreen, L. N. Pfeiffer, K. W. Baldwin, and K. W. West, Phys. Rev. Lett. **77**, 4612 (1996).

[4] L. I. Glazman, I. M. Ruzin, and B. I. Shklovskii, Phys. Rev. B **45**, 8454 (1992).

[5] O. M. Auslaender, H. Steinberg, A. Yacoby, Y. Tserkovnyak, B. I. Halperin, K. W. Baldwin, L. N. Pfeiffer, and K. W. West, Science **308**, 88 (2005).

[6] O. M. Auslaender, A. Yacoby, R. de Picciotto, K. W. Baldwin, L. N. Pfeiffer, and K. W. West, Science **295**, 825 (2002).

[7] Y. Tserkovnyak, B. I. Halperin, O. M. Auslaender, and A. Yacoby, Phys. Rev. Lett. **89**, 136805 (2002).

[8] G. A. Fiete, J. Qian, Y. Tserkovnyak, and B. I. Halperin, Phys. Rev. B **72**, 045315 (2005).

[9] L. N. Pfeiffer, H. L. Stormer, K. W. Baldwin, K. W. West, A. R. Goñi, A. Pinczuk, R. C. Ashoori, M. M. Dignam, and W. Wegscheider, J. Cryst. Growth **127**, 849 (1993).

[10] Y. Tserkovnyak, B. I. Halperin, O. M. Auslaender, and A. Yacoby, Phys. Rev. B **68**, 125312 (2003).

[11] *Single Charge Tunneling: Coulomb Blockade Phenomena in Nanostructures*, NATO ASI Ser. B. Vol. 294, edited by H. Grabert and M. H. Devoret (Plenum Press, New York, 1992).

[12] V. V. Cheianov and M. B. Zvonarev, Phys. Rev. Lett. **92**, 176401 (2004).

[13] G. A. Fiete and L. Balents, Phys. Rev. Lett. **93**, 226401 (2004).